

UC San Diego

UC San Diego Previously Published Works

Title

How turbulence fronts induce plasma spin-up.

Permalink

<https://escholarship.org/uc/item/4ws8q15n>

Journal

Physical review. E, 95(3-1)

ISSN

2470-0045

Authors

Kosuga, Y
Itoh, S-I
Diamond, PH
[et al.](#)

Publication Date

2017-03-29

DOI

10.1103/physreve.95.031203

License

<https://creativecommons.org/licenses/by-nc-nd/4.0/> 4.0

Peer reviewed

How turbulence fronts induce plasma spin-up

Y. Kosuga,^{1,2,*} S.-I. Itoh,^{1,2} P. H. Diamond,³ and K. Itoh^{2,4}

¹Research Institute for Applied Mechanics, Kyushu University, Fukuoka, Japan

²Research Center for Plasma Turbulence, Kyushu University, Fukuoka, Japan

³University of California, San Diego, La Jolla, California 92093, USA

⁴National Institute for Fusion Science, Gifu, Japan

(Received 20 June 2016; revised manuscript received 25 October 2016; published 29 March 2017)

A calculation which describes the spin-up of toroidal plasmas by the radial propagation of turbulence fronts with broken parallel symmetry is presented. The associated flux of parallel momentum is calculated by using a two-scale direct-interaction approximation in the weak turbulence limit. We show that fluctuation momentum spreads faster than mean flow momentum. Specifically, the turbulent flux of wave momentum is stronger than the momentum pinch. The scattering of fluctuation momentum can induce edge-core coupling of toroidal flows, as observed in experiments.

DOI: [10.1103/PhysRevE.95.031203](https://doi.org/10.1103/PhysRevE.95.031203)

The generation of flows by turbulence is widely observed in many systems, including the Sun [1], the planetary atmosphere [2], and toroidal plasmas [3]. While the understanding of the local acceleration mechanisms has been advanced [4], it is now becoming increasingly clear that the nonlocal (global) momentum budget is a key for understanding the overall dynamics [5,6]. For example, the jet sharpening on the planetary atmosphere [2,7] involves not only the local acceleration of flows in the stirring region (the midlatitude on the Earth), but also the response of flows in the equator and the pole regions. In the case of toroidal plasmas [5,6], the change of flows in the main plasmas (i.e., plasmas in the core) mimics that of flows in the peripheral plasmas (i.e., in the edge). In these experiments, flows in the edge plasma reverse its direction upon changing the magnetic geometry, and core flows also systematically respond to the change in edge flows. The experiment implies that edge flows act as a dynamic boundary for core flows, which can be viewed as a case of “the tail wagging the dog” in toroidal plasmas. The entire process can induce the edge-core coupling of toroidal flows.

The purpose of this Rapid Communication is to elucidate the mechanism underpinning the edge-core coupling of toroidal flows in magnetically confined plasmas (Fig. 1). Conventionally, the coupling may be attributed to the inward pinch of edge flows [8,9]. In contrast, here we show that edge and core flows are coupled via the propagation of fluctuation momentum from the edge region into the core region, via a nonlocal process such as turbulence spreading, avalanches, etc. [10–12]. Typically, tokamak plasmas become more turbulent towards the edge with increasing turbulence amplitude [13]. This allows edge turbulence to entrain the core region and to spread parallel fluctuation momentum from the edge to the core plasmas. This effect is captured by nonlinear, triplet flux $\langle \tilde{n} \tilde{v}_r \tilde{v}_\parallel \rangle$, whose contribution is observed in basic experiments [14,15]. The nonlinear flux requires a closure calculation. Recent works [16,17] report the calculations of the nonlinear flux in the strong turbulence regime. However,

the turbulence amplitude is typically at the level of the mixing length estimate, as reported from experiments [18,19] and simulations [20]. Indeed, in many cases of interest, the data overwhelmingly support that the fluctuation amplitude is in the order of or less than the mixing length value. Thus, the Kubo number of turbulence is in the order of unity or less, so that the wave turbulence approach is a more adequate description [21]. In the presence of moderate amplitude drift waves, three-wave resonance sets the necessary phase for spreading [22].

In this Rapid Communication, we present the results for a nonlinear flux in the weak turbulence limit and discuss its role in introducing edge-core coupling of toroidal flows in tokamak plasmas. It is shown that the dominant contribution in the nonlinear flux arises from the three-wave resonance with two small scale waves and one large scale wave (i.e., disparate scale interaction). More importantly, we find that the radial propagation speed of the fluctuation momentum is faster than the inward pinch velocity of mean flow [8,9]. We also find that the resultant torque to drive flows in the core is comparable to that induced by the local (quasilinear) residual stress. Thus, the spreading of fluctuation momentum from the edge to the core plasmas is identified as a relevant mechanism to couple edge-core plasmas by momentum transport. This effect is a key for understanding why “the tail wags the plasma,” i.e., why jogging edge flows by changing magnetic geometry leaves a footprint in the core flow. A perturbative experiment [23–28] is proposed as a further critical test.

To address the issues raised above, here we use an extended version of the Hasegawa-Mima model [29] for drift wave turbulence, with coupling to parallel flows,

$$\frac{d}{dt} (1 - \rho_s^2 \nabla_\perp^2) \frac{e\phi}{T_e} + v_* \partial_y \frac{e\phi}{T_e} + \nabla_\parallel v_\parallel = 0, \quad (1a)$$

$$\frac{d}{dt} v_\parallel = -c_s^2 \nabla_\parallel \frac{e\phi}{T_e}. \quad (1b)$$

Here, $d/dt = \partial_t + (c/B)\hat{z} \times \nabla\phi$ is the total derivative along the $E \times B$ convection. c_s is the ion acoustic speed, v_* is the diamagnetic drift speed, ρ_s is the ion sound Larmor radius, $\nabla_\perp^2 \phi$ is vorticity, and v_\parallel is the parallel ion velocity. \parallel refers to the direction of the magnetic field. \perp corresponds to (r, θ) , which is written as (x, y) locally. Hereafter, we use

*kosuga@riam.kyushu-u.ac.jp

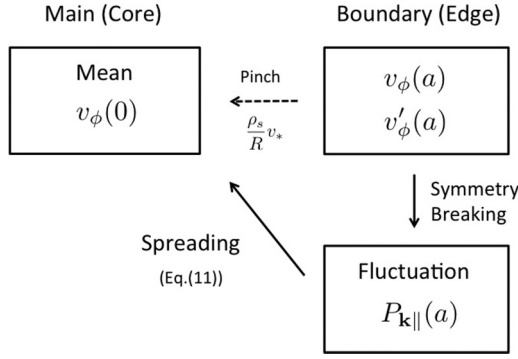


FIG. 1. A schematic picture of the edge-core coupling of toroidal flows. In the conventional view, the change in the mean flow can influence the change in core flows through an inward pinch. Here, in contrast, we argue that the spreading of fluctuation momentum into the core plasmas is a dominant process.

the normalized quantities $\mathbf{x}/\rho_s \rightarrow \mathbf{x}$, $\omega_{ci}t \rightarrow t$, $n_e/n_0 \rightarrow n$, $e\phi/T_e \rightarrow \phi$, $v_{||}/c_s \rightarrow v_{||}$.

Within the model, we consider the evolution of fluctuation momentum density $\langle \tilde{q} \tilde{v}_{||} \rangle$, where $q = (1 - \nabla_{\perp}^2)\phi$. The relation of this term to the parallel fluctuation momentum can be understood by writing it in terms of Fourier components,

$$\langle \tilde{q} \tilde{v}_{||} \rangle = \sum_{\mathbf{k}} (1 + k_{\perp}^2) |\phi_{\mathbf{k}}|^2 \frac{k_{||}}{\omega_{\mathbf{k}}} = \sum_{\mathbf{k}} \mathcal{E}_{\mathbf{k}} \frac{k_{||}}{\omega_{\mathbf{k}}}. \quad (2)$$

Here, $\mathcal{E}_{\mathbf{k}} \equiv (1 + k_{\perp}^2) |\phi_{\mathbf{k}}|^2$ is the energy density of drift waves. By noting that the wave action density is given by $N_{\mathbf{k}} = (1 + k_{\perp}^2) |\phi_{\mathbf{k}}|^2 / \omega_{\mathbf{k}}$, we see that Eq. (2) describes the momentum density of waves $P_{||\mathbf{k}} = k_{||} N_{\mathbf{k}}$ [21,30]. In order for the wave momentum to have a finite value, symmetry breaking in the parallel direction is required [4]. In toroidal plasmas, symmetry can be broken by several mechanisms, such as the intensity gradient, up-down asymmetry [31], the radial electric field, toroidal flow shear [32], etc. Note that toroidal flow shear is important in the edge plasmas, since scrape-off-layer (SOL) flows with a Mach number of order unity are likely to cause a strong radial variation [5].

The wave momentum can be transported spatially. One way to drive wave momentum transport is by the radial propagation of waves [33]. In this case, the radially propagating wave packet carries the momentum. The wave momentum flux is given by $v_{g,x} k_{||} N_{\mathbf{k}}$, with $v_{g,x} = -2k_x k_y v_*/(1 + k_{\perp}^2)^2$ the radial group velocity of drift waves. The wave momentum flux appears as a part of the residual stress. Note that the sign of $k_x k_y$ is determined from the outgoing wave boundary condition [34]. The impact of this property on driving intrinsic torque is discussed in Ref. [35].

In addition to linear propagation, the fluctuation momentum can be nonlinearly scattered and spread in space. This effect is captured by the triplet correlation $\langle \tilde{v}_x \tilde{q} \tilde{v}_{||} \rangle$. A closure calculation is necessary to calculate this term. Here, the closure is done by employing the two-scale direct-interaction approximation [16,22]. In this approach, the nonlinear flux is approximated by the contribution from the beat

term,

$$\langle \tilde{v}_x \tilde{q} \tilde{v}_{||} \rangle \cong \sum_{\mathbf{k}_1 + \mathbf{k}_2 + \mathbf{k}_3 = 0} (\tilde{v}_{x,\mathbf{k}_1}^{(2)} \tilde{q}_{\mathbf{k}_2} \tilde{v}_{||,\mathbf{k}_3} + \tilde{v}_{x,\mathbf{k}_1} \tilde{q}_{\mathbf{k}_2}^{(2)} \tilde{v}_{||,\mathbf{k}_3} + \tilde{v}_{x,\mathbf{k}_1} \tilde{q}_{\mathbf{k}_2} \tilde{v}_{||,\mathbf{k}_3}^{(2)}), \quad (3)$$

where the quantity with the superscript (2) is given by the beat interaction from the two other Fourier components. The beat response [16,21,22] is given by

$$\phi_{\mathbf{k}_1 + \mathbf{k}_2}^{(2)}(t) \cong \int_{-\infty}^t dt' e^{(-i\omega_{\mathbf{k}_1 + \mathbf{k}_2} - |\gamma_{\mathbf{k}_1 + \mathbf{k}_2}^{\text{NL}}|)(t-t')} N_{\mathbf{k}_1 + \mathbf{k}_2}^{\phi(2)}(t'). \quad (4)$$

Here, $\omega_{\mathbf{k}} = \omega_{*e}/(1 + k_{\perp}^2)$ is the frequency of the mode and γ_{NL} is the nonlinear damping rate. $N_{\mathbf{k}_1 + \mathbf{k}_2}^{\phi(2)}$ is the nonlinear term driven by the beating of modes k_1 and k_2 . Explicitly,

$$\begin{aligned} N_{\mathbf{k}_1 + \mathbf{k}_2}^{\phi(2)} = & \frac{\hat{z} \times \mathbf{k}_1 \cdot \mathbf{k}_2 (k_{2\perp}^2 - k_{1\perp}^2)}{2(1 + k_{3\perp}^2)} \phi_{\mathbf{k}_1} \phi_{\mathbf{k}_2} \\ & - \frac{i}{2} \partial_x \phi_{\mathbf{k}_1} \phi_{\mathbf{k}_2} \frac{[k_{2y} (k_{2\perp}^2 - k_{1\perp}^2) + 2k_{1x} \hat{z} \times \mathbf{k}_2 \cdot \mathbf{k}_1]}{(1 + k_{3\perp}^2)} \\ & - \frac{i}{2} \partial_x \phi_{\mathbf{k}_2} \phi_{\mathbf{k}_1} \frac{[k_{1y} (k_{1\perp}^2 - k_{2\perp}^2) + 2k_{2x} \hat{z} \times \mathbf{k}_1 \cdot \mathbf{k}_2]}{(1 + k_{3\perp}^2)}. \end{aligned} \quad (5)$$

The two-scale effect is retained by setting $k_x \rightarrow k_x - i\partial_x$, where k_x denotes the wave number for microscale fluctuation and ∂_x acts on the scale of the envelope. $v_{\mathbf{k}_1 + \mathbf{k}_2}^{(2)}(t)$ is obtained similarly and to the lowest order is given by $v_{\mathbf{k}_1 + \mathbf{k}_2}^{(2)}(t) \cong \{(k_{1||} + k_{2||})/\omega_{\mathbf{k}_1 + \mathbf{k}_2}\} \phi_{\mathbf{k}_1 + \mathbf{k}_2}^{(2)}(t)$. Substituting the beat response into the triplet term, and using the two-time correlation $\langle \phi_{\mathbf{k}}(t) \phi_{\mathbf{k}}^*(t') \rangle = |\phi_{\mathbf{k}}|^2 e^{-i\omega_{\mathbf{k}}(t-t') - |\gamma_{\mathbf{k}}^{\text{NL}}|(t-t')}$, we finally obtain the nonlinear flux as

$$\langle \tilde{v}_x \tilde{q} \tilde{v}_{||} \rangle = \sum_{\mathbf{k}_1} (V_{\mathbf{k}_1} P_{||\mathbf{k}_1} - D_{\mathbf{k}_1} \partial_x P_{||\mathbf{k}_1}). \quad (6)$$

Thus, after the closure calculation, the nonlinear flux is summarized into a compact form, with scale-dependent convection and diffusion. The convection velocity and the diffusion are amplitude dependent, and are given by

$$V_{\mathbf{k}_1} = \partial_x \sum_{\mathbf{k}_2} \theta_{\mathbf{k}_1, \mathbf{k}_2} |\hat{\phi}_{\mathbf{k}_2}|^2 F_1(\mathbf{k}_1, \mathbf{k}_2), \quad (7a)$$

$$D_{\mathbf{k}_1} = \sum_{\mathbf{k}_2} \theta_{\mathbf{k}_1, \mathbf{k}_2} |\hat{\phi}_{\mathbf{k}_2}|^2 F_2(\mathbf{k}_1, \mathbf{k}_2). \quad (7b)$$

Here, ∂_x acts on the envelope scale and $\theta_{\mathbf{k}_1, \mathbf{k}_2}$ is the triad interaction time,

$$\theta_{\mathbf{k}_1, \mathbf{k}_2} = \frac{|\gamma_{\mathbf{k}_1 + \mathbf{k}_2}^{\text{NL}} + \gamma_{\mathbf{k}_1}^{\text{NL}} + \gamma_{\mathbf{k}_2}^{\text{NL}}|}{\Delta\omega_{\text{MM}}^2 + (\gamma_{\mathbf{k}_1 + \mathbf{k}_2}^{\text{NL}} + \gamma_{\mathbf{k}_1}^{\text{NL}} + \gamma_{\mathbf{k}_2}^{\text{NL}})^2}, \quad (8)$$

where $\Delta\omega_{\text{MM}} = \omega_{\mathbf{k}_1 + \mathbf{k}_2} - \omega_{\mathbf{k}_1} - \omega_{\mathbf{k}_2}$ is the mismatch frequency. Note that $\theta_{\mathbf{k}_1, \mathbf{k}_2} \cong \pi \delta(\Delta\omega_{\text{MM}})$ in the wave turbulence limit, which is of interest here. The coupling coefficients F_1

and F_2 are given by

$$F_1(\mathbf{k}_1, \mathbf{k}_2) = \frac{k_{1y}(1 + k_{2\perp}^2)}{4[1 + (\mathbf{k}_1 + \mathbf{k}_2)_\perp^2](1 + k_{1\perp}^2)^2} (-2k_{1x}k_{2x} - 2k_{1y}k_{2y} - k_{2\perp}^2) \{k_{1y}(k_{1\perp}^2 - k_{2\perp}^2 - 2k_{2x}^2) + 2k_{1x}k_{2x}k_{2y}\}, \quad (9a)$$

$$F_2(\mathbf{k}_1, \mathbf{k}_2) = \frac{k_{1y}(1 + k_{2\perp}^2)}{4[1 + (\mathbf{k}_1 + \mathbf{k}_2)_\perp^2](1 + k_{1\perp}^2)^2} (2k_{1x}k_{2x} + 2k_{1y}k_{2y} + k_{2\perp}^2) \{k_{2y}(k_{2\perp}^2 - k_{1\perp}^2 - 2k_{1x}^2) + 2k_{1x}k_{2x}k_{1y}\}. \quad (9b)$$

The convective term $V_{\mathbf{k}_1}$ depends on the triad interaction time, the coupling coefficient, and the intensity profile. Note that in the presence of drift waves, the triad interaction time is approximately $\theta_{\mathbf{k}_1, \mathbf{k}_2} \cong \pi \delta(\Delta\omega_{MM})$. Thus the frequency matching condition is important to produce a nonzero spatial flux. In particular, since the drift waves are dispersive, the matching condition constrains a class of triads that contributes to the nonlinear flux. In order to see this, we have plotted the coupling coefficient F_1 in Fig. 2. Here, $F_1(\mathbf{k}_1, \mathbf{k}_2)$ measures the strength of the coupling from the mode \mathbf{k}_2 to induce the spatial flux of momentum density of the mode \mathbf{k}_1 . The flux is determined by summing over \mathbf{k}_2 , along the three-wave resonant manifold indicated by the red line. Among all possible triads, those that contribute to the flux effectively are also indicated and are given by the coupling among two microscale fluctuations and one fluctuation with a short leg. This class of coupling is called the disparate scale interaction. Finally, a key result here is that for this dominant triad, the coupling coefficient is negative, and is order of unity. The direction of the flux is determined from the combination of this coupling coefficient and the sign of the intensity gradient. For example, if the normalized intensity of the fluctuation increases towards the edge, the convective velocity is inward. This is plausible, since we would expect that the nonlinear flux originates from the region with stronger fluctuation.

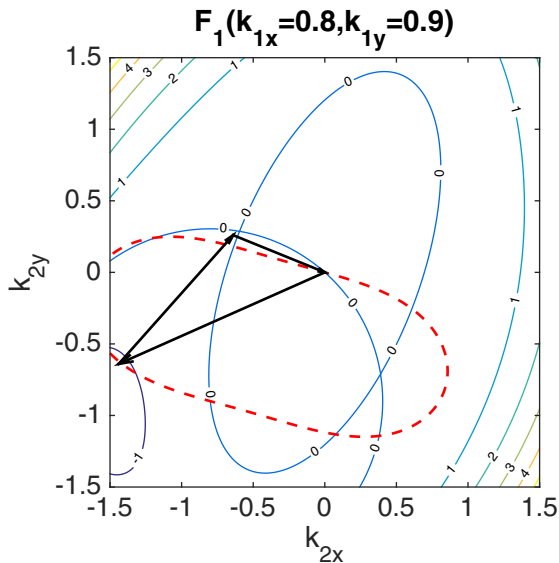


FIG. 2. A contour plot for the coupling coefficient F_1 , for $k_{1x} = 0.8$ and $k_{1y} = 0.9$. The dotted (red) curve is the resonant manifold, defined by $\omega_{\mathbf{k}_1 + \mathbf{k}_2} - \omega_{\mathbf{k}_1} - \omega_{\mathbf{k}_2} = 0$. The summation must be evaluated along the curve. A triad that gives a dominant contribution is also indicated.

We can repeat a similar analysis for the diffusivity $D_{\mathbf{k}} \propto F_2$. In this case, we find that the dominant coupling is due to the disparate scale interaction. The coupling coefficient is of order unity, and the sign is positive. In the sign convention used here, the flux is directed down the gradient, which is the same as the convective piece.

We can summarize the evolution of fluctuation parallel momentum as

$$\partial_t \langle \tilde{q} \tilde{v}_\parallel \rangle + \langle \tilde{q} \nabla_\parallel \tilde{n} \rangle + \partial_x \langle \tilde{v}_x \tilde{q} \tilde{v}_\parallel \rangle = -\langle \tilde{v}_x \tilde{v}_\parallel \rangle \langle n \rangle'. \quad (10)$$

Here, $\langle \tilde{q} \tilde{v}_\parallel \rangle$ is the fluctuation momentum density (in the parallel direction). The second term on the left-hand side is due to the radial propagation of waves, as $\langle \nabla_\perp^2 \tilde{\phi} \nabla_\parallel \tilde{\phi} \rangle \propto \partial_x \sum_{\mathbf{k}} v_{gr,x} k_\parallel \mathcal{E}_{\mathbf{k}} / \omega_{\mathbf{k}}$. The third term is due to turbulence spreading, which is the quantity of interest. After the closure calculation, the nonlinear flux is written in terms of convection diffusion. We note that a similar relation is derived for the fluctuation energy [10,22] and the radial propagation of turbulence is numerically demonstrated. Given the similarity in the mathematical structure, the propagation of fluctuation momentum is very likely.

The major feature of the nonlinear flux is elaborated in the following. Summarizing the above analysis, the nonlinear flux is approximately given by

$$\langle \tilde{q} \tilde{v}_\parallel \tilde{v}_r \rangle \sim -v_* \frac{L_n^2}{\rho_s L_I} |\hat{\phi}|^2 P_{\mathbf{k}_\parallel}. \quad (11)$$

We have restored the dimensional quantities. L_I is the intensity scale length. Here, several caveats follow. First, while in principle the contribution from other waves can accumulate, we retained the contribution from the dominant component, for simplicity. Second, the intensity gradient L_I is that of a normalized fluctuation level. A distinction between the normalized level and absolute level may be important in steep gradient regions. Third, the appearance of L_n is superficial, since the fluctuation amplitude is also a function of L_n . For example, if we invoke the mixing length level estimate, the overall result is

$$\langle \tilde{q} \tilde{v}_\parallel \tilde{v}_r \rangle \sim -v_* \frac{\Delta_c^2}{\rho_s L_I} P_{\mathbf{k}_\parallel}. \quad (12)$$

The dependence on the correlation length Δ_c is plausible, as long-range perturbation (i.e., large Δ_c) leads to larger flux. With these caveats in mind, we discuss the important feature of the nonlinear flux. Here, the sign convention is such that when the fluctuation intensity increases outward, the nonlinear flux is inward. Thus, in typical confined plasmas, the fluctuation momentum can be convected inward from the edge to the core. The typical propagation speed is given by

$$|V_{NL}| \sim v_* \frac{L_n^2}{\rho_s L_I} |\hat{\phi}|^2 \sim v_* \frac{L_s \rho_s}{L_n L_I}. \quad (13)$$

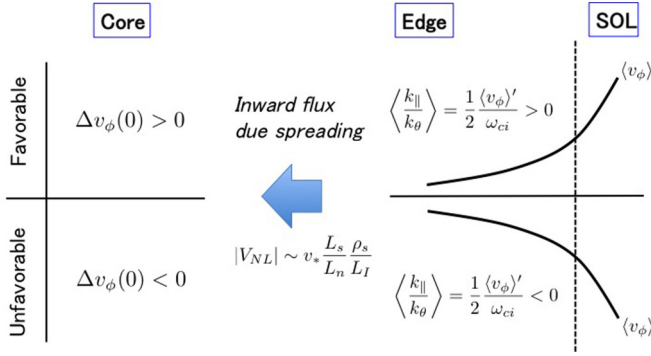


FIG. 3. Jogging the edge flows results in a core flow change by spreading the edge fluctuation momentum into the core.

Here, the amplitude is evaluated from the mixing length estimate $\hat{\phi} \sim \Delta_c/L_n$ with $\Delta_c = \sqrt{L_s/L_n}\rho_s$. The propagation velocity is then typically around the diamagnetic speed. Note that the propagation velocity is faster than the inward pinch velocity of mean momentum, $V_{\text{pinch}} \sim D/R \sim v_*(\rho_s/R)$, where the gyro-Bohm diffusivity $D \sim \rho_s v_*$ is assumed. For typical parameters, the ratio is

$$\frac{|V_{\text{NL}}|}{|V_{\text{pinch}}|} \sim \frac{RL_s}{L_I L_n} \gg 1. \quad (14)$$

Thus fluctuation momentum is scattered into the core before the mean momentum is pinched in. This effect can be important for the fast response of the core to the edge perturbation, the edge-core coupling of toroidal flows, etc., as discussed in detail later. Finally, we note that the resultant nonlinear stress can be compared to the quasilinear stress as

$$\frac{|\Pi_{r\parallel}^{\text{triple}}|}{|\Pi_{r\parallel}^{\text{QL}}|} \sim \frac{|V_{\text{NL}}|}{|v_{\text{gr}}|} \sim \frac{1}{\rho_s^2 k_\theta k_r} \frac{L_s \rho_s}{L_n L_I}. \quad (15)$$

For the nonlinear term to be comparable to the quasilinear term, the intensity gradient scale length needs to be shorter than $L_I \sim (L_s/L_n)\Delta_c$, where $k_r \sim \Delta_c^{-1}$ was assumed.

The nonlinear flux can induce the edge-core coupling of toroidal flows (Fig. 3). Here, for simplicity, we assume that fluctuation energy can propagate from the edge to the core, although a more detailed analysis will be required to characterize the radial extent. As an example, we consider the correlation between core toroidal flows and edge magnetic geometry [5,6]. When the magnetic drift is toward the x point of the magnetic separatrix, namely, for a favorable configuration, SOL flows are in the codirection and the edge toroidal flow shear is positive [5,36]. In this case, the positive toroidal flow at the edge breaks the parallel symmetry [32] to yield fluctuation momentum in the codirection $\langle P_{k\parallel} \rangle \propto \langle k_{\parallel}/k_{\theta} \rangle \propto \langle v_{\phi} \rangle' |_{a} > 0$. This fluctuation momentum can be scattered into the core via the spreading process, and can result in a coincrement in the core flow. This is consistent

with the observation [6], which indicates that the core toroidal flows are less in the counterdirection (sometimes in the codirection) in the favorable configuration. When we change the magnetic geometry from the favorable to the unfavorable configuration, SOL flows and edge toroidal flow shear change their sign, and consequently the fluctuation momentum is in the counterdirection $\langle P_{k\parallel} \rangle \propto \langle k_{\parallel}/k_{\theta} \rangle \propto \langle v_{\phi} \rangle' |_{a} < 0$. This can be scattered into the core to accelerate toroidal core flows in a more counterdirection. Thus, the spreading of fluctuation momentum in the edge can be a key for understanding the observed edge-core coupling of toroidal flows.

Another important consequence that the nonlinear flux can induce is the dynamic response of the core flows against the edge perturbation [23–28]. As discussed above, the nonlinear flux allows the fluctuation momentum to propagate faster than the mean momentum. This process can result in a fast response of the core flows against the edge perturbation, with the response time shorter than the confinement time. The typical response time is estimated as $\tau_{\text{res}} \sim a/|V_{\text{NL}}| \sim (L_I/\sqrt{L_s L_n})\tau_E \ll \tau_E$. The fast response can be tested by perturbative experiments, using pellet injection, etc., with a fast time resolution charge exchange for toroidal flows in the core. Repetitive perturbation and conditional averaging may be useful as well. Finally, we note that repetitive perturbation will be required to induce steady change in the core flow.

In summary, we find that turbulence can scatter fluctuation momentum in the edge plasmas into the core plasmas to induce the edge-core coupling of toroidal flows (Fig. 1). The process was formulated by calculating the nonlinear flux of fluctuation momentum. The closure calculation via a two-scale direct-interaction approximation (TSDIA) in the weak turbulence limit gives the nonlinear flux [Eq. (6)], which scales as $\sim -v_*[L_n^2/(\rho_s L_I)]|\hat{\phi}|^2 P_{\parallel \mathbf{k}}$. The flux is down the intensity gradient. Since the fluctuation intensity increases toward the edge in typical fusion plasmas, the nonlinear flux describes *inward* propagation of fluctuation momentum from the edge. The effective propagation velocity of fluctuation momentum is faster than the inward pinch velocity. Hence, we identify the inward flux of fluctuation momentum as a dominant process to couple edge and core plasmas in toroidal momentum transport. This process can be a key for understanding why jogging edge flows results in the change of the core toroidal flows, as reported in experiments (Fig. 3).

We thank Dr. Lu Wang, Dr. Z. B. Guo, Professor K. Ida, Professor A. Fujisawa, Professor S. Inagaki, Dr. T. Kobayashi, Dr. K. J. Zhao, and the participants in the Festival de Theorie for stimulating discussions. This work is partly supported by Grants-in-Aid for Scientific Research of JSPS of Japan (JP15K17799, JP15H02155, JP16H02442), Asada Science Foundation, Kyushu University Interdisciplinary Programs in Education and Projects in Research Development (26705), and Kyushu University QR Research Program (28315).

[1] G. Rüdiger, *Differential Rotation and Stellar Convection* (Gordon and Breach, New York, 1989).

[2] G. K. Vallis, *Atmospheric and Oceanic Fluid Dynamics* (Cambridge University Press, Cambridge, U.K., 2006).

- [3] K. Ida and J. E. Rice, *Nucl. Fusion* **54**, 045001 (2014).
- [4] P. H. Diamond, Y. Kosuga, O. D. Gürcan, C. J. McDevitt, T. S. Hahm, N. Fedorczak, J. E. Rice, W. X. Wang, S. Ku, J. M. Kwon *et al.*, *Nucl. Fusion* **53**, 104019 (2013).
- [5] B. LaBombard, J. E. Rice, A. E. Hubbard, J. W. Hughes, M. Greenwald, J. Irby, Y. Lin, B. Lipschultz, E. S. Marmor, C. S. Pitcher *et al.*, *Nucl. Fusion* **44**, 1047 (2004).
- [6] J. Rice, A. C. Ince-Cushman, M. L. Reinke, Y. Podpaly, M. J. Greenwald, B. LaBombard, and E. S. Marmor, *Plasma Phys. Controlled Fusion* **50**, 124042 (2008).
- [7] D. G. Dritschel and M. E. McIntyre, *J. Atmos. Sci.* **65**, 856 (2008).
- [8] T. S. Hahm, P. H. Diamond, Ö. D. Gürcan, and G. Rewoldt, *Phys. Plasmas* **14**, 072302 (2007).
- [9] M. Yoshida, Y. Kamada, H. Takenaga, Y. Sakamoto, H. Urano, N. Oyama, and G. Matsunaga (the JT-60 Team), *Phys. Rev. Lett.* **100**, 105002 (2008).
- [10] X. Garbet, L. Laurent, A. Samain, and J. Chinardet, *Nucl. Fusion* **34**, 963 (1994).
- [11] S. Ku, J. Abiteboul, P. H. Diamond, G. Dif-Pradalier, J. M. Kwon, Y. Sarazin, T. S. Hahm, X. Garbet, C. S. Chang, G. Latu *et al.*, *Nucl. Fusion* **52**, 063013 (2012).
- [12] F. Hariri, V. Naulin, J. J. Rasmussen, G. S. Xu, and N. Yan, *Phys. Plasmas* **23**, 052512 (2016).
- [13] A. E. White, L. Schmitz, G. R. McKee, C. Holland, W. A. Peebles, T. A. Carter, M. W. Shafer, M. E. Austin, K. H. Burrell, J. Candy *et al.*, *Phys. Plasmas* **15**, 056116 (2008).
- [14] B. Labit, C. Theiler, A. Fasoli, I. Furno, and P. Ricci, *Phys. Plasmas* **18**, 032308 (2011).
- [15] S. Inagaki, T. Kobayashi, Y. Kosuga, S.-I. Itoh, T. Mitsuzono, Y. Nagashima, H. Arakawa, T. Yamada, Y. Miwa, N. Kasuya *et al.*, *Sci. Rep.* **6**, 22189 (2016).
- [16] L. Wang, T. Wen, and P. H. Diamond, *Phys. Plasmas* **22**, 052302 (2015).
- [17] L. Wang, T. Wen, and P. H. Diamond, *Nucl. Fusion* **56**, 106017 (2016).
- [18] C. M. Surko and R. E. Slusher, *Science* **221**, 817 (1983).
- [19] G. R. McKee, C. C. Petty, R. E. Waltz, C. Fenzi, R. J. Fonck, J. E. Kinsey, T. C. Luce, K. H. Burrell, D. R. Baker, E. J. Doyle *et al.*, *Nucl. Fusion* **41**, 1235 (2001).
- [20] B. D. Scott, *Phys. Rev. Lett.* **65**, 3289 (1990).
- [21] P. H. Diamond, S.-I. Itoh, and K. Itoh, *Modern Plasma Physics Volume 1: Physical Kinetics of Turbulent Plasmas* (Cambridge University Press, Cambridge, U.K., 2011).
- [22] O. D. Gurcan, P. H. Diamond, and T. S. Hahm, *Phys. Plasmas* **13**, 052306 (2006).
- [23] K. W. Gentle, W. L. Rowan, R. V. Bravenec, G. Cima, T. P. Crowley, H. Gasquet, G. A. Hallock, J. Heard, A. Ouroua, P. E. Phillips, D. W. Ross, P. M. Schoch, and C. Watts, *Phys. Rev. Lett.* **74**, 3620 (1995).
- [24] M. W. Kissick, J. D. Callen, and E. D. Fredrickson, *Nucl. Fusion* **38**, 821 (1998).
- [25] P. Mantica, P. Galli, G. Gorini, G. M. D. Hogeweij, J. de Kloe, N. J. Lopes Cardozo, and RTP Team, *Phys. Rev. Lett.* **82**, 5048 (1999).
- [26] S. Inagaki, N. Tamura, T. Tokuzawa, K. Ida, K. Itoh, S. V. Neudatchin, K. Tanaka, Y. Nagayama, K. Kawahata, M. Yakovlev, S. Sudo, and the LHD Experimental Group, *Plasma Phys. Controlled Fusion* **48**, A251 (2006).
- [27] S. Hong-Juan, D. Xuan-Tong, Y. Liang-Hua, F. Bei-Bin, L. Ze-Tian, D. Xu-Ru, and Y. Qing-Wei, *Plasma Phys. Controlled Fusion* **52**, 045003 (2010).
- [28] J. E. Rice, C. Gao, M. L. Reinke, P. H. Diamond, N. T. Howard, H. J. Sun, I. Cziegler, A. E. Hubbard, Y. A. Podpaly, W. L. Rowan *et al.*, *Nucl. Fusion* **53**, 033004 (2013).
- [29] A. Hasegawa and K. Mima, *Phys. Fluids* **21**, 87 (1978).
- [30] B. B. Kadomtsev, in *Reviews of Plasma Physics*, edited by V. Shafranov (Kluwer Academic, New York, 2001), Vol. 22.
- [31] Y. Camenen, Y. Idoumura, S. Jolliet, and A. G. Peeters, *Nucl. Fusion* **51**, 073039 (2011).
- [32] X. Garbet, C. Fenzi, H. Capes, P. Devynck, and G. Antar, *Phys. Plasmas* **6**, 3955 (1999).
- [33] P. H. Diamond, C. J. McDevitt, Ö. D. Gürcan, T. S. Hahm, and V. Naulin, *Phys. Plasmas* **15**, 012303 (2008).
- [34] L. D. Pearlstein and H. L. Berk, *Phys. Rev. Lett.* **23**, 220 (1969).
- [35] C. J. McDevitt, P. H. Diamond, O. D. Gurcan, and T. S. Hahm, *Phys. Rev. Lett.* **103**, 205003 (2009).
- [36] N. Fedorczak, P. H. Diamond, G. Tynan, and P. Manz, *Nucl. Fusion* **52**, 103013 (2012).